SIZE, SOLUBILITY, AND THE SEROTONIN-GATED ION CHANNEL RECEPTOR: IN SEARCH OF AN IMPROVED EXTRACELLULAR DOMAIN MODEL

A Senior Scholars Thesis

by

EMILY SARAH WEISS

Submitted to the Office of Undergraduate Research
Texas A&M University
in partial fulfillment of the requirements for the designation as

UNDERGRADUATE RESEARCH SCHOLAR

April 2009

Majors: Biochemistry
Genetics

SIZE, SOLUBILITY, AND THE SEROTONIN-GATED ION CHANNEL RECEPTOR: IN SEARCH OF AN IMPROVED EXTRACELLULAR DOMAIN MODEL

A Senior Scholars Thesis

by

EMILY SARAH WEISS

Submitted to the Office of Undergraduate Research
Texas A&M University
in partial fulfillment of the requirements for the designation as

UNDERGRADUATE RESEARCH SCHOLAR

Approved by:

Research Advisor: Gregg B. Wells
Associate Dean for Undergraduate Research: Robert C. Webb

April 2009

Majors: Biochemistry
Genetics

ABSTRACT

Size, Solubility, and the Serotonin-gated Ion Channel Receptor: In Search of an Improved Extracellular Domain Model. (April 2009)

Emily Sarah Weiss
Department of Biochemistry/Biophysics
Texas A&M University

Research Advisor: Dr. Gregg B. Wells
Department of Molecular and Cellular Medicine

The 5-HT_3 receptor (5-HT_3R) is the only serotonin receptor that is not a G-coupled protein receptor. It has been implicated as a contributor to cytotoxic drug-evoked emesis, irritable bowel syndrome, pruritis, schizophrenia, Parkinson disease, addiction, bulimia, nociception, and problems with cognitive function. It follows that improved, more specific 5-HT_3R antagonists are an attractive goal for the pharmaceutical industry. Current models of the 5-HT_3R are based on homology to the highly structurally related and well studied nicotinic acetylcholine receptor, but no high resolution image of the full length 5-HT_3R has yet been determined. This research works towards development of an extracellular domain model, which would be a better candidate for x-ray crystallography and NMR spectroscopy due to its higher water solubility and smaller size. Constructs of the mouse 5-HT_3R were made with an N-terminal mAb-142 epitope

tag for immunoblotting with a linker region to promote flexibility of the tag in the extracellular domain. A Kozak sequence was incorporated to optimize expression in *Xenopus* oocytes. Designs included a full length construct; a construct truncated after the first transmembrane domain with valine substituted for an intra-membrane aspartic acid residue; and constructs terminated after the extracellular domain, after the first transmembrane domain, and directly preceding the third transmembrane domain. Binding assays with [^{3}H]-granisetron showed significant binding only with the full length construct, though minimal binding was observed with the construct with the valine substitution. These results suggest that elements present in the other parts of the native receptor may be vital to efficient ligand binding and should be included in the design of a successful truncated model.

DEDICATION

To all of my grandparents, Elly and Grant Risch and Tony and Shelia Hiscocks.

ACKNOWLEDGMENTS

First of all, I would like to thank my research advisor, Dr. Gregg B. Wells, not only for his incredible support of this project, but also for his instrumental contributions to my personal development as a scientist. I cannot recall one instance in which Dr. Wells was ever unwilling to put aside what he was doing in order to help me discover a solution to a problem. The opportunity to work under such a patient, committed advisor is not one that many undergraduates are able to have and is one for which I am incredibly grateful.

I would also like to thank Alexi Person for her guidance and friendship. The knowledge I have gained from her will last me throughout my career. Alexi's constant willingness to help has been instrumental in the completion of this project, and I am sincerely appreciative of her generosity and hard work.

Through the course of my undergraduate career, I am very fortunate to have been influenced by Dr. Scott Jacques's never-ending optimism, kindness, and curiosity. He has been such a helpful mentor and is a constant source of inspiration for me. Dr. Roger Buchanan has also been a wonderful teacher throughout the years I have known him; my positive, earliest laboratory experiences at the Arkansas Biosciences Institute were pivotal towards establishing my desire to pursue research.

Lastly, I would like to thank my friends and family for their continued love and support. Katherine and Ian have been there for me throughout everything; I am lucky to have such delightful people as my closest friends. I am grateful to Kevin, for his unfailing energy, optimism, and encouragement. My dad, Tom, has been such an inspiration, and being exposed to his research throughout my youth has had quite an impact on me. I am also thankful to my sister, Hannah, and, of course, to Mum, for their love and support.

NOMENCLATURE

5-HT_3	5-Hydroxytryptamine
5-HT_3R	5-HT_3 Receptor
ACh	Acetylcholine
AChBP	Acetylcholine Binding Protein
ECD	Extracellular Domain
GABA	γ-Aminobutyric Acid
LGIC	Ligand-Gated Ion Channel
M1	First Transmembrane Domain
nAChR	Nicotinic Acetylcholine Receptor
NMR	Nuclear Magnetic Resonance

TABLE OF CONTENTS

Page

Page

LIST OF FIGURES

LIST OF TABLES

CHAPTER I

INTRODUCTION: THE 5-HT_{3A} RECEPTOR AS A TARGET FOR THERAPEUTIC AGENTS

Ionotropic receptors are ligand-gated ion channels (LGICs) that respond to the binding of neurotransmitters such as acetylcholine (ACh), 5-hydroxytryptamine (5-HT_3), glycine, or γ-aminobutyric acid (GABA). Binding of the appropriate ligand causes an increased probability of conformational change of the receptor, channel opening, and the exchange of specific ions across the membrane. The generation of a membrane potential depends upon changes of ion concentrations across the membrane; LGICs are, therefore, vital to rapid chemical transmission of nerve impulses.

Structure and classification of the 5-HT_3R

The Cys-loop superfamily of LGICs consists of both anionic-selective inhibitory receptors which cause hyperpolarization of the membrane (including those activated by GABA or glycine) and cation-selective excitatory receptors which cause depolarization of the membrane (including those activated by ACh or 5-HT_3). Members of this superfamily of receptors share several distinguishing features. The five protein subunits that compose a Cys-loop receptor are arranged about a central pore which is permeable

This thesis follows the style of *Journal of Biological Chemistry*.

to ions. Relative permeability of sodium, potassium, and calcium vary depending on the specificity of the individual receptor.

Each subunit has a ligand-binding N-terminal extracellular domain (ECD) containing a characteristic thirteen residue sequence. This sequence is bordered on either side by cysteine residues, which form a disulfide bond and create a closed loop localized between the binding and channel domains (1). The channel domain consists of four transmembrane spanning helices (designated M1-M4), with M2 lining the pore and M1, M3, and M4 comprising the outer helices (2). Cys-loop receptors are widely dispersed throughout the central and peripheral nervous systems. Because of the quantity of unique subunits and their ability to co-assemble with numerous subunits in a variety of different pentamers, ligand binding properties and pharmacological profiles of Cys-loop receptors are incredibly diverse.

The cation-selective Cys-loop receptors

There are at least seven serotonin (5-HT) receptor subclasses, but the 5-HT_3 receptors (5-HT_3Rs) are the only type which are LGICs; the others are G-protein coupled receptors, which are not classified as part of the Cys-loop superfamily (3). The most widely studied family of the Cys-loop superfamily is that of the nicotinic acetylcholine receptor (nAChR). These LGICs open in response to nicotine as well as to ACh. NAChR research has been favored because of the general biological availability of the nAChR through isolation of muscle-type nAChR from *Torpedo* ray, the fairly recent

discovery of ACh binding protein (AChBP), a protein with a homologous extracellular domain to that of the nAChR, and the discovery of a wide range of snake toxins which aid in the purification of nAChRs (Figure 1). The structure of the 5-HT_3Rs, on the other hand, is not resolved at a high resolution, though it is widely accepted to be similar to that of the nAChR. Various homology models have been proposed (4).

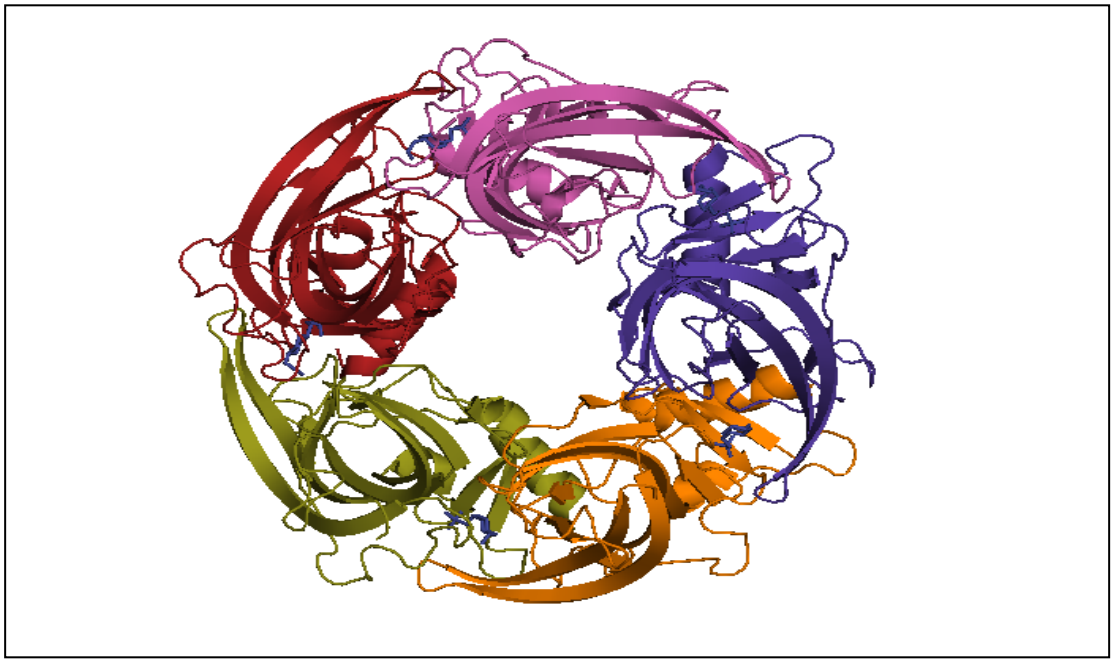

FIGURE 1. **Model of AChBP.** Model generated in PyMol from 2.7 Å X-ray crystallography structure of AChBP (Protein Data Bank entry DOI 10.2210/pdb1i9b/pdb).

Classes of 5-HT_3Rs

Two 5-HT_3R subunits (subunits A and B) have been characterized most thoroughly. The 5-HT_{3A} subunits assemble as homopentamers, and also as heteropentamers with the 5-HT_{3B} subunit, which does not itself form homopentamers (5). The 5-HT_{3C}, 5-HT_{3D},and

5-HT_{3E} subunits have recently been found to form heteropentamers with the 5-HT_{3A} subunit, but these heteropentamers do not exhibit markedly different pharmalogical profiles than that of 5-HT_{3A} homopentamers (6). The 5-HT_{3A} receptor can also assemble with some nAChR subunits to form heteromeric receptors. Combining 5-HT_{3A} subunits with the nAChR α4 subunit produces a particularly novel heteropentamer with increased calcium ion permeability and reduced sensitivity to the antagonist tubocurarine (7).

Distribution and therapeutic targeting

5-HT_{3A} receptor subunit mRNA has been discovered in numerous brain regions and in the small intestine, colon, spleen, thymus, and prostate (8). In addition, 5-HT_{3AB} receptors are expressed in many cells of the immune system, pointing to a possible role in inflammation (9). 5-HT_{3B} receptor subunit mRNA is less ubiquitous, but has been detected primarily in brain and kidney by Northern blot analysis (10). 5-HT_3R concentration is highest in the brain regions (especially the brain stem) but is also significant in the gastrointestinal tract where the receptors contribute to regulation of the enteric nervous system (11).

Associated pathologies

5-HT_3Rs have been implicated in a wide variety of disorders. The mechanism of radiation-induced emesis involves the release of serotonin and its direct effect upon the 5-HT_3R (12). This mechanism has led to the use of 5-HT_3R antagonists as a treatment for the adverse side effects of chemotherapy, as well as for nausea and vomiting due to

surgery or pregnancy. It has been proposed that the 5-HT_3R boasts a role in the mediation of inflammatory pain, making pharmaceutical studies of antagonists as nociceptives similarly attractive (13). The G-protein coupled 5-HT receptors have been associated with an vast variety of behavioral disorders such as general anxiety disorders, social phobias, obsessive-compulsive disorders, panic disorders, and post traumatic stress disorders (14). 5-HT_3 antagonists in particular have anti-psychotic effects in patients with Parkinson disease and improve p50 gating in schizophrenics (15-18). Irritable bowel syndrome may be caused in part by abnormal function of 5-HT_3Rs, but antagonists have only been an effective treatment in women (19). In addition, the 5-HT_3R possesses a significant role in cognitive function, and there is some evidence that antagonists could be helpful in the treatment of addiction, bulimia, and pruritis (18). Taking into account the myriad of disorders associated with the 5-HT_3R, it is not difficult to appreciate the advantages presented by fully understanding the workings of the 5-HT_3R and designing antagonists with better selectivity and activity.

Models of the 5-HT_3R

The most definitive breakthroughs in the field of Cys-loop receptor research have come through the discovery and isolation of AChBP from the freshwater snail *Lymnaea stagnalis*. AChBP is a water-soluble homopentamer with ACh binding sites and has subunits featuring a twelve-membered Cys-loop (instead of thirteen-membered) and similar size and shape to the ECD of the *Torpedo* nAChR. Since its structure was first determined by x-ray crystallography in 2001, crystal structures of AChBP at numerous

resolutions in the range of 2.9 Å and with various ligands bound to the active site have been visualized (20-24).

Another breakthrough was the electron microscopy of the *Torpedo* ray muscle nAChR. Though the resolution of this image was only 4 Å, the spatial relationships between the binding and channel domains, the protein backbone, and the locations of α-carbon atoms and bulky side chains were ascertained (2). Recently, the first atomic resolution crystal structure of a monomeric nAChR ECD at a resolution of 1.94 Å has been determined (25).

Modeling of the 5-HT_3R at this point is based solely on homology to elucidated structures of AChBP and nAChRs; a high resolution image of the 5-HT_3R itself is yet to be obtained. Discovering more detail about the structure and function of the 5-HT_3R and its subunits would facilitate the design of novel therapeutic agents and promote more refined treatments for the considerable number of 5-HT_3R-related pathologies.

Benefits of an ECD model

One strategy to further illuminate the structure of the 5-HT_3R is to develop a model which is more water soluble. A more water soluble protein will crystallize more easily and therefore be a better candidate for x-ray crystallography. Wells et. al have underscored the utility of creating an ECD model of the nAChR, which, because of its shorter length, would additionally be a better candidate for nuclear magnetic resonance

spectroscopy (NMR) (26). Though various ECD models of nAChRs have been produced, they have been limited in simulating ligand binding affinities and subunit assembly. An ECD model that more closely reflects the properties of the full-length receptor remains a very attractive objective for both the nAChR and the 5-HT_3R.

Illuminating the role of M1

The presence of M1 is necessary for efficient expression of extracellular α7 nAChRs (27) as well as for α4β2 nAChRs (26). It has been proposed that M1 functions primarily as a tether (28), but roles in surface trafficking (29) and channel gating(30) in nAChRs and as a primary determinant of desensitization kinetics in 5-HT_3Rs (31) have also been proposed.

This study probes the importance of M1 in efficient functioning of extracellular 5-HT_3Rs. The role of an atypical hydrophilic residue present in M1 is explored. Elucidating the function of M1 in the 5-HT_3A receptor subunit will aid in the creation of a more representative truncated model of the 5-HT_3R.

CHAPTER II

METHODS

Construction of 5-HT_{3A} DNA plasmids

Primer design

Sequences were introduced into plasmids using modified QuikChange PCR. Point mutations and additions of three or fewer bases were incorporated into primers and plasmids using a standard QuikChange mutagenesis procedure.

Description of constructs

The *Xenopus* Kozak sequence (ACC) was inserted directly before the start codon of the sequence coding for the mouse full length 5-$HT3_A$ subunit in the pSP64 poly(A) plasmid (32). The starting full length construct, a gift from David Julius, originally contained two copies of the mAb 142 epitope at the C-terminus. Using two rounds of modified QuikChange PCR, an N-terminus mAb 142 epitope (QVTGEVIFQTPLIKNP) surrounded on either side by a linker region (consisting of 6 repeats of alanine, guanine, and serine) was inserted into the ECD (33). DNA sequences were optimized for expression using GeneDesign 2.0 and the codon usage table for *Xenopus laevis*. To halt the translation of the two C-terminal epitope tags, the first base pair of the first tag was mutated to a uracil, generating a UAA stop codon. This construct was designated 5-HT_3Full.

The 5-HT_3M1, 5-HT_3ECD, and 5-HT_3M1M2 constructs were derived from the 5-HT_3Full construct using PCR mutagenesis. To produce the 5-HT_3M1 construct, a stop codon was inserted two amino acids after the end of the first transmembrane domain. The 5-HT_3ECD construct was produced by insertion of a stop codon directly before the start of M1. The 5-HT_3M1M2 construct was produced by insertion of a stop codon directly preceding the third transmembrane domain. The 5-$HT_3$970V construct was derived from the 5-HT_3M1 construct and contained a substitution of an aspartic acid residue in the interior of M1 to a valine residue (Figure 2). Primers for PCR mutagenesis were ordered from Invitrogen, subjected to PAGE purification, and reconstituted at a concentration of 20 pmol/µl (Table 1).

PCR

PCR with AccuPrime™ *Pfx* DNA polymerase (Invitrogen) was carried out using 10 ng of template DNA, 50 picomoles of each primer, and 5 µl AccuPrime™ *Pfx* Reaction Mix. After denaturation for 3 minutes at 95°C, the reaction tube underwent 25 cycles of denaturation at 95°C for 1 minute, annealing at 53-68°C for 1 minute, and extension at 72°C for 10 minutes.

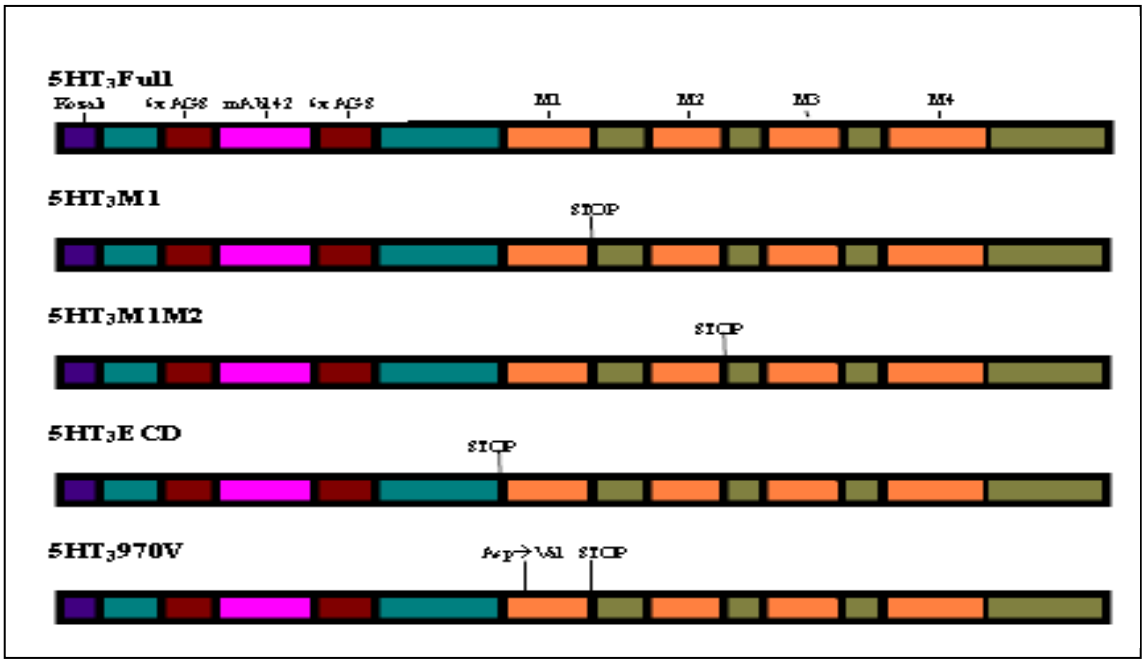

FIGURE 2. **Schematics of 5-HT$_3$R construct design.** The Kozak fragment (purple) directly precedes the ECD (teal). Each linker region (maroon) consists of alanine, guanine, and serine (repeated 6 times). The mAb 142 epitope binding region (magenta) is between 2 linker AGS repeat regions. The transmembrane segments (orange) are situated between other coding segments (olive). The location of inserted stop codons for various constructs is indicated. Valine has been substituted for an aspartic acid residue as shown in 5HT3970V.

TABLE 1	
Primers for creation of $5HT_{3A}$ constructs	
Adding Xenopus Kozak fragment	FORWARD: 5'- GAATACAAGCTTGCCACCATGCGGCTCTGCATCCCGCAGGTGC -3' REVERSE: 5'- GATGCAGAGCCGCATGGTGGCAAGCTTGTATTCTATAGTGTCACC -3'
First linker and first half of mAb 142 epitope tag	FORWARD: 5'- TCTGCTGGATCTGCAGGTTCAGCCGGATCCCAAGTGACAG GAGAAGTTATCTTTACCCAGCCTGCTCTACTAAGGCTGTCAGAC-3' REVERSE: 5'- GGATCCGGCTGAACCTGCAGATCCAGCAGAACCAGCACTT CCGGCACTCCCAGCGGTATCTCGGGCCTGGGTGGCCCTCCTCCG-3'
Second half of mAb 142 epitope tag and second linker	FORWARD: 5'-GCAGGGAGCGCCGGCAGCGCAGGATCAGCAGGCTCCGCTGG TAGCGCTGGCTCTACCCAGCCTGCTCTACTAAGGCTGTCAGAC-3' REVERSE: 5'- TGCTGATCCTGCGCTGCCGGCGCTCCCTGCAGGGTTCTTAATCA ATGGAGTCTGAAAGATAACTTCTCCTGTCACTTGGGATCC-3'
Removing C-terminal 2x mAb 142 epitope	FORWARD: 5-GGCATTATTCTACGCGTTAAGTAACAGGAGAAGTAATCTTCC-3' REVERSE: 5'-CTTCTCCTGTTACTTAACGCGTAGAATAATGCCAAATGGACC-3'
5-HT_3 M1	FORWARD: 5'-CTGCCCCCGGACAGTTGAGAGAGAGTCTCTTTCAAGATCACAC-3' REVERSE: 5'-GAAAGAGACTCTCTCTCAACTGTCCGGGGGCAGGCAAAAGCCC-3'
5-HT_3 M1M2	FORWARD: 5'-GCCATCGGTACCTAACCCCTCATTGGTGTCTACTTTGTGG-3' REVERSE: 5'- ACACCAATGAGGGGTTAGGTACCGATGGCCGTTGCCGGCAG-3'
5-HT_3 ECD	FORWARD: 5'-ATCCGCCGGAGGTAGCCTTTATTCTATGCAGTCAGCCTCTTGC-3' REVERSE: 5'- CATAGAATAAAGGCTACCTCCGGCGGATGATCACGTAGAAC-3'
5-HT_3 970V	FORWARD: 5'-TCCTCATGGTCGTGGTCATTGTGGGCTTTTGCCTGCCCCCG-3' REVERSE: 5'-CAAAAGCCCACAATGACCACGACCATGAGGAAGATACTGGG-3'

PCR product purification

The PCR product was run at 97 volts on a 1% agarose gel containing 1µL/mL ethidium bromide at room temperature in 1X TAE buffer. Correct PCR product was selected and

digested at 37°C with Dpn I for 2 hours to degrade parent DNA. After heat inactivation at 80°C for 20 minutes, the product was run on a 1% agarose gel under the above mentioned conditions. The desired band was extracted using the Zymoclean Gel DNA Recovery Kit.

Bacterial transformation

One Shot OmniMAX 2 T1 Phage-Resistant Cells (Invitrogen) were incubated for 30 minutes with 2 µl of DNA product after thawing on wet ice for 30 minutes. They were heat shocked for 1 minute at 42°C and placed on ice again for 5 minutes. After shaking at 225 rpm for 30 minutes at 37°C in LB medium, the bacterial solution was centrifuged at 14000 rpm for 2 minutes. The bacterial pellet was resuspended in 50 µL of LB containing 0.5 µL of ampicillin. Dilutions of 1:1, 1:10, and 1:100 of the reaction were spread onto LB plates containing ampicillin and grown at 37°C overnight.

Purification and isolation of DNA

Colonies were selected and added to 2-3 mL of LB containing 2-3 µL ampicillin and grown overnight. DNA was isolated and purified using the Zyppy Plasmid Mini-prep procedure. Double digests were performed with EcoRV and Xho I at 37°C with Buffer 3 + BSA to confirm presence of correct plasmid. After sequencing, a colony known to contain the correct plasmid was chosen from a bacterial stock plate and added to a flask containing 200 mL of LB and 200 µL ampicillin; the bacteria was grown overnight, and DNA was isolated using the QIAGEN Plasmid Midi-Prep Kit. Double and single

digests were performed with EcoRV and/or Xho I to confirm presence of correct DNA and to determine concentration.

Expression of protein in *Xenopus* oocytes

Ten µg of DNA was linearized by incubation for 3 hours with EcoRI at 37°C and recovered via a phenol/chloroform extraction and ethanol precipitation. RNA was produced from linearized DNA using an SP6 mMessage mMachine Kit and recovered through phenol/chloroform extraction and precipitation with isopropanol. The product was verified by running on a 1% agarose gel.

Xenopus laevis were obtained from NASCO (Fort Atkinson, WI) and cared for in a manner approved by the Institutional Animal Care and Use Committee of Texas A&M University. After removal from the frog by survival surgery, oocytes were rinsed with calcium-free OR2, defolliculated with collagenase 1A, and rotated gently to aid in separation. After rinsing in Leibovitz's L- glutamine medium powder (L-15) + HEPES, oocytes were stored in L-15 at 19°C until injection.

Oocytes were selected for injection based upon color and division. Approximately 41 nL of RNA was oil hydraulically delivered with a glass capillary into the oocyte cytoplasm. After injection, the oocytes were incubated at 19°C for three days in L-15, 10 units/mL penicillin, 10 µg/mL streptomycin, and 10 µg/mL gentamycin.

After homogenizing oocytes in wash buffer (50 mM NaH_2PO_4, 50 mM NaCl, 5 mM EDTA, and 5 mM EGTA) containing protease inhibitors (5 mM benzamidine and 15 mM iodoacetamide), protein was isolated by centrifugation for 30 minutes. The supernatant was removed, and the pellet resuspended in extraction buffer + 2% Triton with protease inhibitors and rotated for 2 hours. After further centrifugation, the supernatant protein extract was removed and used for immunoblotting and ligand binding assays.

Immunoblotting

After deglycosylation with PNGase F, the samples were denatured at 95ºC for 5 minutes and then run on a 12.5% acrylamide gel at room temperature and 30 mA. Using a GENIE box, the protein was transferred to an Immun-Blot™ (Bio—Rad) polyvinylidene difluoride membrane at 30 volts for 30 minutes with 1X Western blot transfer buffer. The membrane was blocked overnight with gentle rocking at 4°C with dry milk in a PBS/0.05% TWEEN 20 solution. After overnight incubation at 4°C and constant rocking with the primary antibody mAb 142 in block at a ratio of 1:10,000, the membrane was washed three times for an hour each with 1X PBS/0.05% TWEEN solution. The membrane was incubated overnight at 4°C in a 1:5,000 ratio of secondary antibody, Goat anti Rat. The wash steps were repeated and the membrane was developed on BioMax ML film using SuperSignal West Dura Extended Duration Substrate.

Ligand binding assays

Immulon 4 HBX flat bottom polystyrene microtiter strips (Thermo Labsystems) were incubated overnight with 100 µL of 10 mM CAPSO containing 4 µg/mL mAb 142 at 4°C in sealed plastic. After washing three times with NaN_3-PBS, they were incubated with 250 µL per well of PBS/NaN_3-BSA blocker for approximately 3 hours at 4°C. Wells were then washed three times with wash buffer + 2% Triton X-100. Protein extract was added to wells in duplicate in concentrations of ¼ oocyte and 1 oocyte, using extraction buffer + 2% Triton containing protease inhibitors to bring to a total concentration of 100 µL per well. After incubation overnight at 4°C with constant rocking, wells were washed three times with wash buffer + 2% Triton.

Twenty-five µCi of granisetron (Perkin Elmer Cat # NET-1030 BRL-43694, [9-methyl-^{3}H]-) was purchased at a concentration of 1.0 mCi/mL and with a specific activity of 85.3 Ci/mmol. Granisetron was added to wells at a concentration of 5 nM per well in 100 µL of extraction buffer + 2% Triton following safety protocols for use of radioactive substances. After incubation at 4°C overnight in sealed plastic, the wells were washed with wash buffer + 2% Triton and shaken at room temperature for 30 minutes with 120 µL per well of 5% SDS + 25 mM DTT in extraction buffer + 2% Triton. Liquid was removed from wells and placed in 3 mL of scintillation fluid (FISHER ScintiSafe Econo 1 LSC-Cocktail) in 6 mL polyethylene vials (Packard BioScience). Radioactivity was counted on a Packard 2500TR Liquid Scintillation Analyzer.

CHAPTER III

RESULTS

Production of plasmids

To insert longer DNA sequences into plasmids, a modified QuikChange PCR strategy was used. Primers were designed so that after incorporation of new sequence, ends of the DNA would overlap and a "pseudo-circle" could be formed. This is important so that the DNA, which is linear after PCR, can be taken up and propagated as circular plasmids by bacteria.

First, each primer contained approximately 30 bases complementary to the other primer in the pair. This allows for creation of the "pseudo-circle." These 30 base pairs were "new," but repeated in both primers. Next, up to 20 new bases could be incorporated into each primer, allowing for about 40 new base pairs in all in the product DNA. Finally, each primer contained 30 base pairs complementary to the template DNA in order to facilitate binding to the template. In this manner, it was possible to incorporate up to 70 new base pairs in the product DNA in one round of PCR. The desired product was generated from about 50% of the clones.

The Kozak sequence has been shown to be a significant contributing factor to optimization of protein expression (32). The Kozak sequence for *Xenopus* (ACC) was successfully inserted through the use of PCR mutagenesis.

Using two additional rounds of PCR, the N-terminal mAb 142 epitope tag, surrounded on either side by a "linker" region, was inserted into the ECD. Each linker region consisted of an alanine, glycine, and serine segment repeated six times. The linker regions were incorporated to promote flexibility of the epitope tag binding region in the ECD, thereby improving antibody binding and reducing possible interference with the ligand binding domain.

Epitope binding regions inserted in the C-terminus of 5-HT_3R constructs have been determined to interfere with ligand binding in truncated constructs despite abundant protein production. For this reason, a final round of PCR mutagenesis was performed and a stop codon was inserted directly preceding the two C-terminal copies of the mAb 142 epitope tag binding region present in the starting receptor.

For all constructs, the PCR product with the highest yield of DNA at the appropriate base pair length (4686 to 4774 base pairs, depending on the construct) was chosen for digestion with Dpn I to degrade parent DNA (Figure 3).

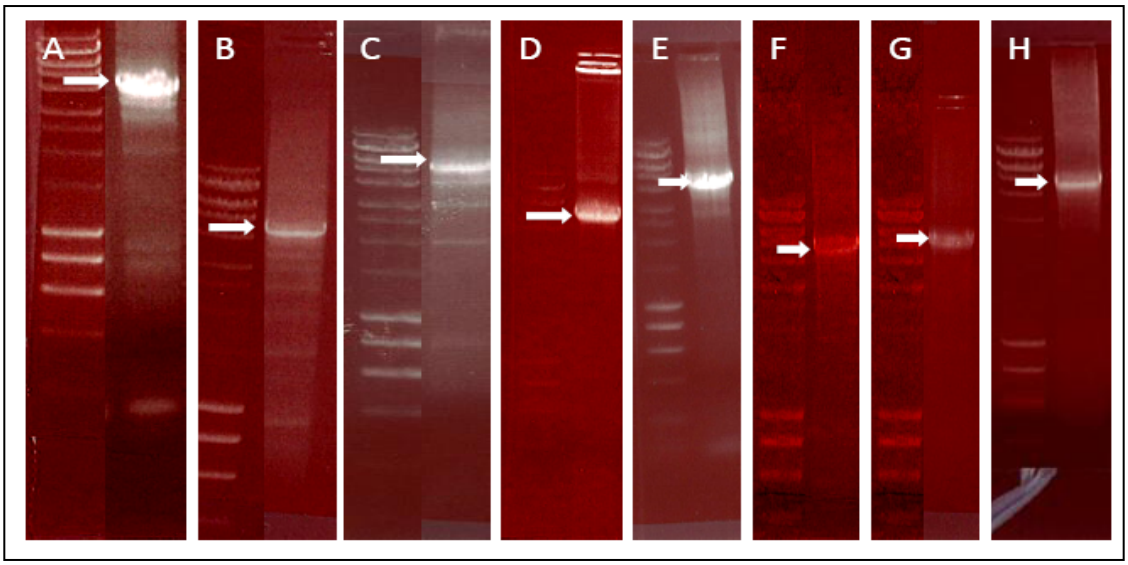

FIGURE 3**. PCR products chosen for Dpn I digestion.** Desired band is marked with a white arrow. DNA ladders from each respective gel are shown. *A.* First round of PCR to insert linker region and mAb142 epitope. *B.* Second round inserting linker and epitope. *C.* Insertion of Kozak fragment. *D.* Insertion of stop codon before C-terminal epitope tags. *E.* 5-HT_3M1. *F.* 5-$HT_3$970V. *G.* 5-HT_3M1M2. *H.* 5-HT_3ECD.

Extraction after running on an agarose gel allowed for purification of the product; a representation of a Dpn I digested sample is shown with the band marked which was extracted (Figure 4).

DNA amplification in bacteria

Colonies grown from dilutions of 1:1, 1:10, and 1:100 of the transformed bacteria were chosen based on size and resolution from other colonies for plasmid DNA extraction via mini-prep (Figure 5). Colonies were round and pale white.

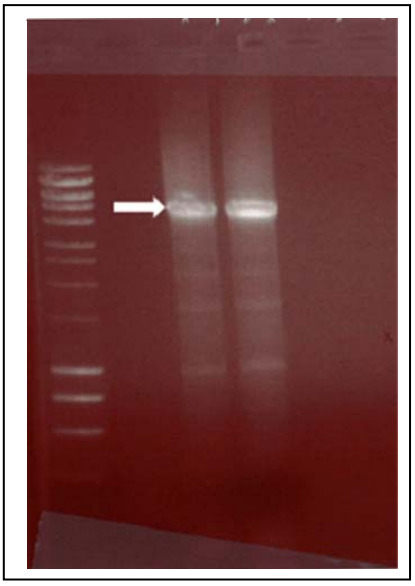

FIGURE 4**. Extraction of Dpn I digested sample.** Extracted band from digested sample of second round of PCR to insert linker region and mAb142 epitope. Chosen band is marked with a white arrow.

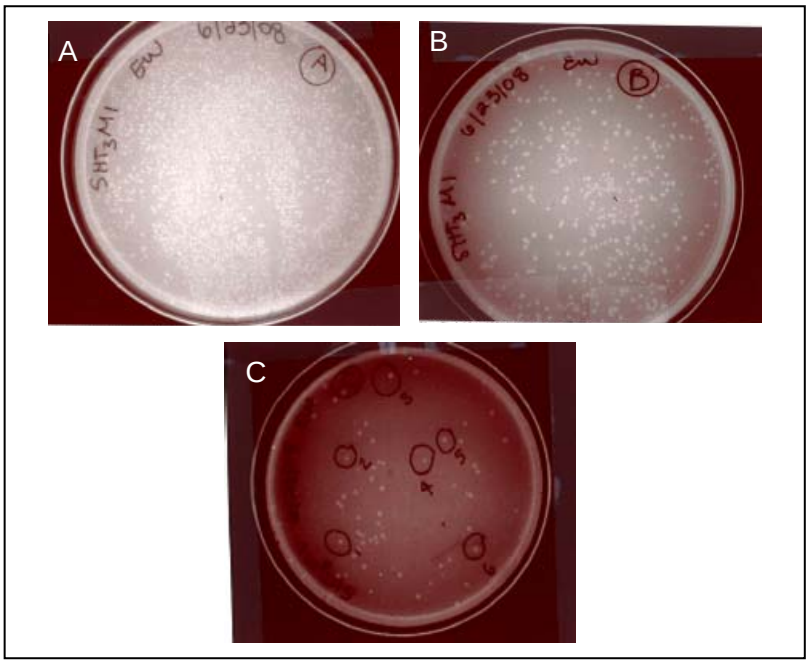

FIGURE 5. **Plates of bacteria transformed with the 5-HT$_3$M1 plasmid.** *A.* Colonies grown from a 1:1 dilution of transformed bacterial solution, *B.* a 1:10 dilution, and *C.* a 1:100 dilution. For bacteria transformed with the 5-HT$_3$M1 plasmid, all colonies were selected from plate C. Colonies were chosen based on regularity of shape and resolution from other colonies.

Double digests performed with EcoRV and Xho I at 37°C with Buffer 3 + BSA confirmed presence of correct plasmid based on prediction of band size; correct plasmids from mini-preps were sequenced (Figure 6).

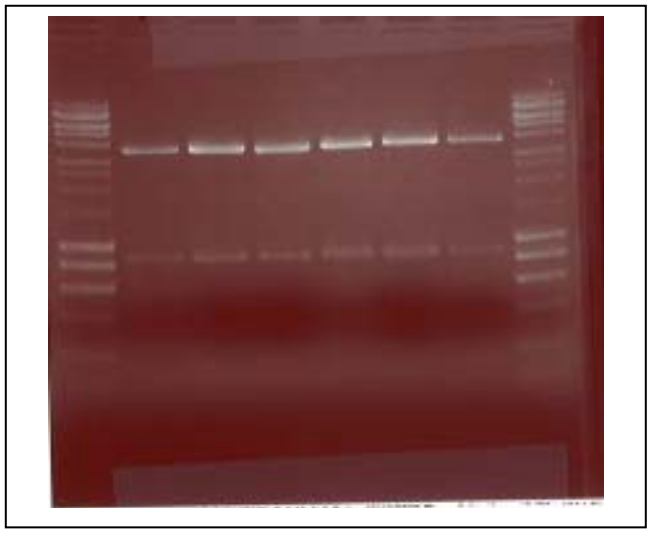

FIGURE 6. **Double digest of mini-preps for sequencing.** Shown is the double digest of 5-HT3Full after the first round of PCR. DNA from lanes 2,3,4, and 5 were sequenced to confirm correct DNA. Bands with lengths of 886 and 3882 base pairs confirm the presence of 5-HT3Full.

Double and single digests were performed on midi-prep products with EcoRV and/or Xho I to confirm presence of correct DNA and to determine concentration (Figure 7). DNA yield was sufficient for all constructs and yielded approximately 50 µL DNA at concentrations in the range of 0.08 µg/µL to 0.500 µg/µL.

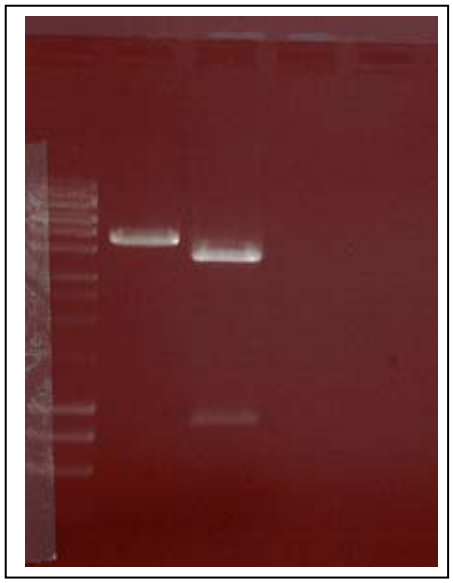

FIGURE 7. **Double and single digests of midi-prep.** Shown are the single digest of 5-HT3Full with EcoRV after insertion of the Kozak sequence (lane 1) and the double digest with EcoRV and Xho I to confirm correct DNA plasmid (lane 2). The concentration was estimated to be 0.08 µg/µL based on comparison with the DNA marker.

Protein expression

DNA was successfully linearized and RNA produced from all constructs (Figure 8). After injection of RNA in oocytes and production and extraction of protein, the supernatant protein extract was removed and used for immunoblotting and ligand binding assays. The desired protein was shown by Western blot analysis to be successfully produced from all constructs (Figure 9).

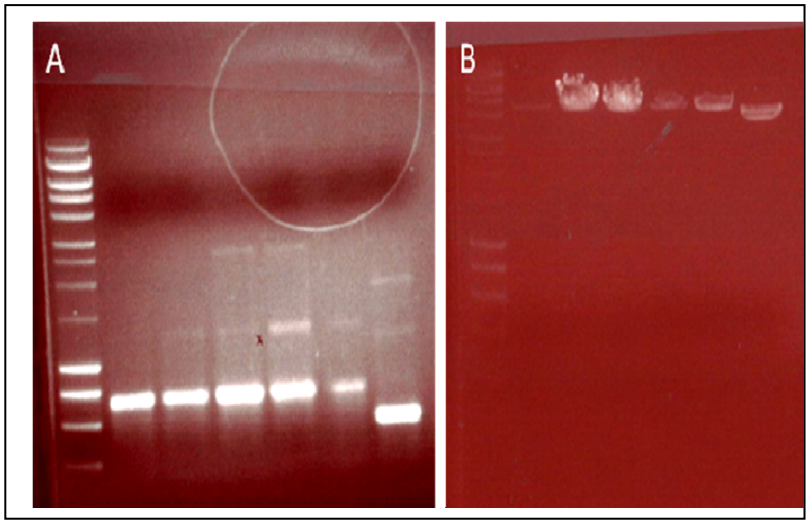

FIGURE 8. **RNA production from construct DNA.** *A.* RNA production from linearized DNA using an SP6 mMessage mMachine Kit. From left to right are $5HT_3$Full, $5HT_3$M1, $5HT_3$ECD, $5HT_3$M1M2, $5HT_3$970V, and the control, $5HT_3$M1 C-term 2x mAb 142 (a construct containing 2 copies of a C-terminal epitope tag, previously determined to bind antibody for Western blotting but to have limited ligand binding activity). *B.* Linear DNA from incubation with EcoRI. From left to right are $5HT_3$Full, $5HT_3$M1, $5HT_3$970V, $5HT_3$ECD, $5HT_3$M1M2, and control.

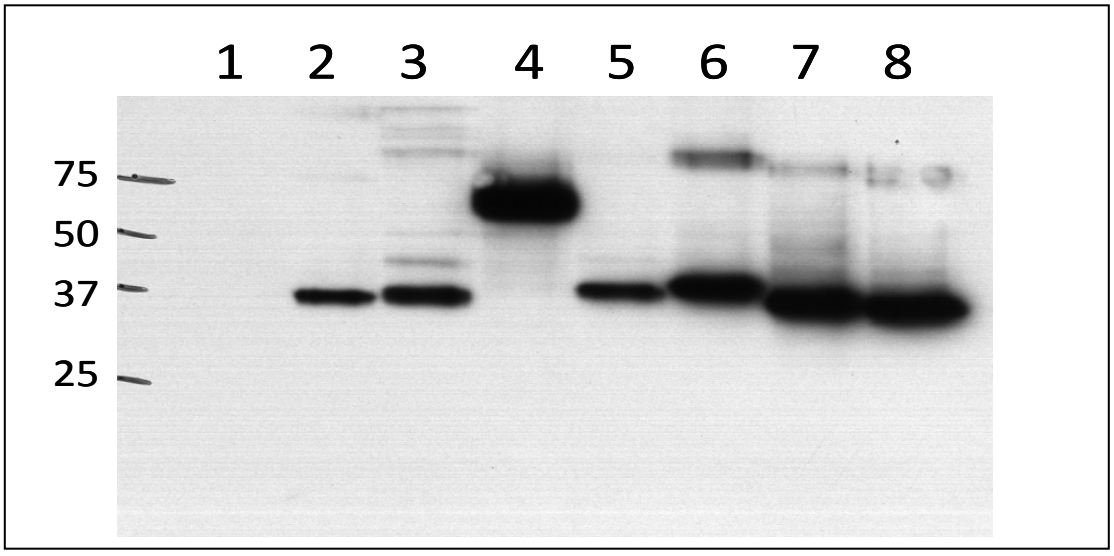

FIGURE 9. **Immunoblot of protein from constructs.** Protein was expressed successfully for all constructs in yields comparable to that of the full length. Shown is protein from uninjected oocytes (1), α4M1 2x142 + βM1236 control (2), 5-HT_3M1 2xmAb142 C-term control (3), 5-HT_3Full (4), 5-HT_3M1(5), 5-HT_3M1M2 (6), 5-$HT_3$970V (7), and $5HT_3$ECD (8). Protein from 1/6 oocyte (3.37 µL) was loaded for all samples except for uninjected (1 oocyte at 20.2 µL).

Western blots exhibited a minimum amount of background noise. Because the additional proteins did not move as far as the target proteins, they were surmised to have originated due either to incomplete denaturation or to insufficient deglycosylation. No extraneous proteins were observed in the lane containing the uninjected oocytes. This supports the conclusion that the extra bands were not due to contamination or insufficient purification of the extract from the oocytes. Two controls were also run on the Western blot and similarly exhibited the extra bands. Because of these results, it is all the more likely that the variations in protein size are due to incomplete denaturation or deglycosylation.

Ligand binding

Previous studies with the nAChR have shown that ECD models truncated before M1 exhibit compromised ligand binding, but those truncated after M1 exhibit comparable ligand binding to that of the native receptor (26). Because of this, it was anticipated that the 5-HT_3ECD construct would similarly exhibit highly reduced ligand binding, but that the 5-HT_3M1 construct would bind to granisetron.

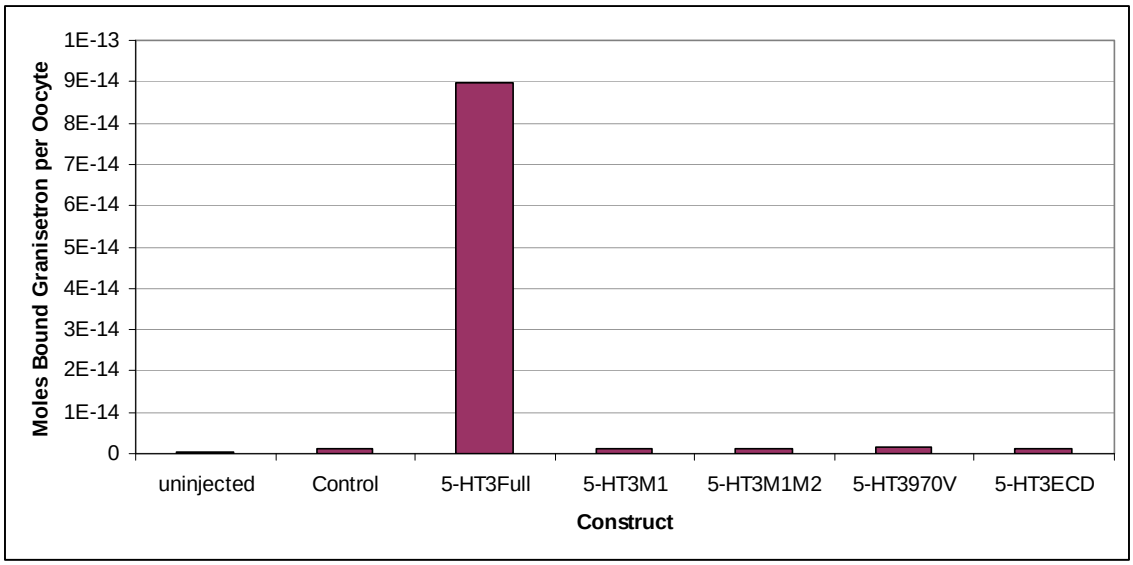

FIGURE 10. **Binding of granisetron to construct protein.** None of the constructs displayed ligand binding profiles comparable to that of the full-length. The 5-HT_3M1 2xmAb142 C-term construct was used as the control. Moles of bound granisetron was determined as an average of moles bound per oocyte from assays run in duplicate in concentrations of ¼ and 1 oocyte.

As predicted, the 5-HT_3ECD construct did not show significant binding compared to the 5-HT_3Full construct (Figure 10). Negligible binding to granisetron of the 5-HT_3M1 construct, however, was unexpected. This finding points to the essential function of other portions of the receptor or to a conformational change or other interference of the ligand binding site on exposure of M1.

Amino acid residues located in a transmembrane spanning segment of a protein are generally characterized by having uncharged side chains; this promotes stability in the hydrophobic interior of a membrane's lipid bilayer. The middle region of the first transmembrane domain of the 5-HT_3R contains aspartic acid, an acidic residue. Because

the mutation of a corresponding aspartic acid residue in M1 of the nAChR to a nonpolar amino acid enhances ligand binding, it was proposed that this acidic aspartic acid residue may interact with another basic residue localized elsewhere in a transmembrane domain of the protein for neutralizing the negative charge of the aspartic acid side chain and efficient assembly of the subunits. A likely basic residue is K281 near the start of M2. This motivated design of the 5-HT_3M1M2 and 5-$HT_3$970V constructs. It was proposed that if a corresponding basic residue (such as K281) interacts with M1 in the native conformation of the receptor, the 5-HT_3M1M2 construct would exhibit successful binding. Mutation of the aspartic acid to a nonpolar residue, such as valine in the construct 5-$HT_3$970V, would eliminate the need for interaction with another residue, allowing for increased binding to granisetron.

Significant binding was not observed for the 5-HT_3M1M2 construct, however. Though minimal binding was recorded for the 5-$HT_3$970V construct, there was not enough evidence to sustain the hypothesis that exposure of the aspartic acid residue in M1 causes interference with the ligand binding site (Figure 10).

CHAPTER IV

SUMMARY AND CONCLUSIONS

Unlike the nAChR, truncation after the first transmembrane domain of the 5-HT_3R does not yield a receptor with comparable ligand binding properties to that of the full length receptor. Because of the amount of homology between the nAChR and the 5-HT_3R, it was expected that, as for the nAChR, truncating the receptor before the start of M1 would not yield an ECD model with an at least partially equivalent ligand binding profile to that of the native receptor, but that truncation after M1 would produce a receptor with a similar binding profile.

An aspartic acid situated in the middle of M1 is present in both the 5-HT_3R and the nAChR. Considering that mutation of the aspartic acid residue to an uncharged residue in a truncated nAChR leads to increased binding, a suitable hypothesis was able to be proposed concerning the lack of increased binding for similarly truncated 5-HT_3R constructs: (1) that this charged amino acid, positioned in the midst of a hydrophobic region, was either interacting with another residue and had an important role in creating a certain conformation for the formation of a ligand binding site, or (2) that by removing a residue which in the native conformation was interacting with the aspartic acid, the exposed residue was producing conformational changes inhibiting the binding site.

To determine the extent of the influence of this particular amino acid in the functioning of the native receptor, a construct was created including M2, which contains a basic lysine residue, in addition to M1. The inclusion of M2 would help restore the binding site, if this was, in fact, the role of the aspartic acid in question. It must be noted, however, that by truncating the receptor after M2, a negative charge from the carboxyl group of the terminal amino acid may have been introduced into the vicinity of the binding site, causing unintentional, ancillary interactions. Perhaps a construct designed that places the terminal amino acid within the membrane would lead to improved binding to granisetron of the 5-HT_3M1M2 construct.

Another construct, substituting the aspartic for a nonpolar amino acid, valine, also was created. In this construct, the removal of the charge from M1 would facilitate the formation of the binding site if the exposed negative charge from the aspartic acid buried in the membrane was the cause of aberrant folding of the subunit and reduced ligand binding.

Surprisingly, none of the constructs (excepting the full length construct) exhibited appreciable ligand binding. Though the 5-$HT_3$970V construct did show minimal binding, it was nevertheless severely reduced compared to that of the full length construct. From this it must be concluded that either the exposure of the aspartic acid residue does not significantly affect the binding abilities of the receptor as it does in the nAChR, or the more likely explanation, that the absence of a distinct, vitally important

region present in the native receptor 5-HT_3R is severely inhibiting the ligand binding capacity of the receptor.

It has been proposed that the C-terminus of the 5-HT_3R performs a critical role in the function of the native receptor. In their search to identify the minimum number of residues needed to create the binding site, Butler *et. al* have emphasized the role of the short extracellular 5-HT_3R C-terminus in the formation of a functional, homomeric 5-HT_3A receptor, mostly in subunit folding and maturation (34). Deletion of the terminal alanine led to 4% ligand binding compared to the wild type receptor. Mutations of this alanine to other small, nonpolar amino acids such as valine, glycine, and leucine also reduced radioligand binding. Substitution to alanine of the two amino acids immediately preceding the terminal alanine (glutamine and tyrosine) did not inhibit binding. A role for the C-terminus in "locking" the receptor in a mature binding conformation, through interaction of the tyrosine with the Cys-loop of the N-terminus, has also been proposed by Pons *et. al* (35). This group further postulates that the mature conformation, by concealing a retention signal present in M1, allows for proper export of the receptor to the cell surface.

Due to the role of the 5-HT_3R in a large variety of pathologies, including cytotoxic drug-evoked emesis, schizophrenia, Parkinson disease, addiction, and nociception, the elucidation of its structure remains an invaluable objective. Though these findings did not clarify a role for the aspartic acid in the midst of M1, further work in this direction

would be beneficial. Inclusion of part of the C-terminus may prove to have drastically beneficial effects on ligand binding profiles in later studies. With this addition, it may be possible to revisit the question of the importance of M1 to receptor function. This would be a considerable contribution towards the design of a shorter, more soluble ECD model with which a high resolution structure of the 5-HT_3R may finally be attained.

REFERENCES

1. Sine, S. M., and Engel, A. G. (2006) *Nature* **440**, 448-455

2. Miyazawa, A., Fujiyoshi, Y., and Unwin, N. (2003) *Nature* **423**, 949-955

3. Reeves, D. C., and Lummis, S. C. R. (2002) *Mol. Membr. Biol.* **19**, 11-26

4. Thompson, A. J., and R. Lummis, S. C. (2006) *Curr. Pharm. Design* **11**, 527-540

5. Barnes, N. M., Hales, T. G., Lummis, S. C. R., and Peters, J. A. *Neuropharmacology* **In Press, Corrected Proof**

6. Niesler, B., Kapeller, J., Hammer, C., and Rappold, G. (2008) *Pharmacogenomics* **9**, 501-504

7. van Hooft, J. A., Spier, A. D., Yakel, J. L., Lummis, S. C. R., and Vijverberg, H. P. M. (1998) *Proc. Natl. Acad. Sci. U.S.A.* **95**, 11456-11461

8. Miyake, A. M. S., Takemoto, Y., and Akuzawa, S. (1995) *Mol. Pharmacol.* **48**, 407-416

9. Fiebick, B. L., Seidel, M., Geyer, V., Haus, U., Muller, W., Stratz, T., and Candelario-Jalil, E. (2004) *Scand. J. Rheumatol. Suppl.*, 9-11

10. Davies, P. A., Pistis, M., Hanna, M. C., Peters, J. A., Lambert, J. J., Hales, T. G., and Kirkness, E. F. (1999) *Nature* **397**, 359-363

11. Galligan, J. J. (2002) *Neurogastroent. Motil.* **14**, 611-623

12. Feyer, P. C., and Titlbach, O. J. (1998) *Supportive Care in Cancer* **6**, 253-260

13. Costall, B., and Naylor, R. J. (2004) *Current Drug Targets* **3**, 27-37

14. Jones, B. J., and Blackburn, T. P. (2002) *Pharmacol. Biochem. Be.* **71**, 555-568

15. Zoldan, J., Friedberg, G., Livneh, M., and Melamed, E. (1995) *Neurology* **45**, 1305-1308

16. Adler, L. E., Cawthra, E. M., Donovan, K. A., Harris, J. G., Nagamoto, H. T., Olincy, A., and Waldo, M. C. (2005) *Am. J. Psychiatry* **162**, 386-388

17. Koike, K., Hashimoto, K., Takai, N., Shimizu, E., Komatsu, N., Watanabe, H., Nakazato, M., Okamura, N., Stevens, K. E., Freedman, R., and Iyo, M. (2005) *Schizophr. Res.* **76**, 67-72

18. Thompson, A. J., and Lummis, S. C. R. (2007) *Expert Opin. Ther. Targets* **11**, 527-540

19. Camilleri, M. (2000) *Expert Opin. Inv. Drug* **9**, 147-159

20. Brejc, K., van Dijk, W. J., Klaassen, R. V., Schuurmans, M., van der Oost, J., Smit, A. B., and Sixma, T. K. (2001) *Nature* **411**, 269-276

21. Bourne, T. T., Hansen, S. B., Taylor, P., and Marchot, P. (2005) *EMBO J.* **24**, 1512-1522

22. Celie, P. H. N., Kasheverov, I. E., Mordvintsev, D. Y., Hogg, R. C., van Nierop, P., van Elk, R., van Rossum-Fikkert, S. E., Zhmak, M. N., Bertrand, D., Tsetlin, V., Sixma, T. K., and Smit, A. B. (2005) *Nat. Struct. Mol. Biol.* **12**, 582-588

23. Ihara, O. T., Yamashita, A., Oda, T., Hirata, K., Nishiwaki, H., Morimoto, T., Akamatsu, M., Ashikawa, Y., Kuroda, S., Mega, R., Kuramitsu, S., Satelle, D., and Matsuda, K. (2008) *Invert. Neurosci.* **8**, 71-81

24. Brejc, K., Smit, A. B., and Sixma, T. K. (2002) *Novartis Found. Symp.* **245**, 22-29

25. Dellisanti, C. D., Yao, Y., Stroud, J. C., Wang, Z. Z., and Chen, L. (2007) *Nat. Neurosci.* **10**, 953-962

26. Person, A. M., Bills, K. L., Liu, H., Botting, S. K., Lindstrom, J., and Wells, G. B. (2005) *J. Biol. Chem.* **280**, 39990-40002

27. Wells, G. B., Anand, R., Wang, F., and Lindstrom, J. (1998) *J. Biol. Chem.* **273**, 964-973

28. Wang, Z. Z., Hardy, S. F., and Hall, Z. W. (1996) *J. Biol. Chem.* **271**, 27575-27584

29. Wang, J. M., Zhang, L., Yao, Y., Viroonchatapan, N., Rothe, E., and Wang, Z. Z. (2002) *Nat. Neurosci.* **5**, 963-970

30. Gleitsman, K. R., Kedrowski, S. M. A., Lester, H. A., and Dougherty, D. A. (2008) *J. Biol. Chem.*

31. Lobitz, N., Gisselmann, G., Hatt, H., and Wetzel, C. H. (2001) *Mol. Pharmacol.* **59**, 844-851

32. van der Velden, A. W., Voorma, H. O., and Thomas, A. A. M. (2001) *Biotechniques* **31**,

33. Boyd, G. W., Doward, A. I., Kirkness, E. F., Millar, N. S., and Connolly, C. N. (2003) *J. Biol. Chem.* **278**, 27681-27687

34. Butler, A. S., Lindesay, S. A., Dover, T. J., Kennedy, M. D., Patchell, V. B., Levine, B. A., Hope, A. G., and Barnes, N. M. (2009) *Neuropharmacology* **56**, 292-302

35. Pons, J. S., Bourgeois, J. P., Taly, A., Changeux, J. P., and Devillers-Thiéry, A. (2004) *Eur. J. Neurosci.* **20**, 2022-2030

CONTACT INFORMATION

Name:	Emily Sarah Weiss
Professional Address:	c/o Dr. Gregg B. Wells Department of Molecular and Cellular Medicine 440 Reynolds Medical Building Texas A&M University College Station, TX 77843-1114
Email Address:	weisse@tamu.edu
Education:	B.S., Biochemistry, Genetics Texas A&M University, May 2010 Undergraduate Research Scholar